Terahertz broadband polarizer using bilayer subwavelength metal wire-grid structure on polyimide film

Xiao Wu (吴 晓)[1], Huayue Li (李化月)[1], Shixiong Liang (梁士雄)[2], Jianjun Liu (刘建军)[1], Zhanghua Han (韩张华)[1], and Zhi Hong (洪 治)[1*]

[1]*Centre for THz Research, China Jiliang University, Hangzhou 310018, China*
[2]*Science and Technology on ASIC Laboratory, Hebei Semiconductor Research Institute, Shijiazhuang 050051, China*
[*]*Corresponding author: hongzhi@cjlu.edu.cn*

Received August 29, 2014; accepted November 14, 2014; posted online December 22, 2014

A terahertz (THz) broadband polarizer using bilayer subwavelength metal wire-grid structure on both sides of polyimide film is simulated by the finite-difference time-domain method. We analyze the effect of film thickness, material loss, and lateral shift between two metallic gratings on the performance of the THz polarizer. Bilayer wire-grid polarizers are fabricated by a simple way of laser induced and non-electrolytic plating with copper. The THz time-domain spectroscopy measurements show that in 0.2–1.6 THz frequency range, the extinction ratio is better than 45 dB, the average extinction ratio reaches 53 dB, and the transmittance exceeds 67%, which shows great advantage over conventional single wire-grid THz polarizer.

OCIS codes: 230.5440, 040.2235.
doi: 10.3788/COL201513.012303.

With the rapid development of terahertz (THz) technology, especially the THz radiation and detecting technology[1], applications of THz wave in various areas, such as spectroscopy, imaging, sensing, and detection were greatly enhanced[2–7]. As one of the quasi-optical devices to manipulate the THz waves, the demand for high-performance THz polarizers is increasing. Recently, several kinds of polarizers, such as Brewster angle reflection polarizers[8], liquid crystal polarizers[9], and wire-grid polarizers[10] are widely used in THz field. Brewster angle reflection polarizer can only work at the specific angle of incidence. Liquid crystal polarizer has a good performance of polarization, but a narrow operating frequency range (0.2–1.0 THz) limits its application. Free-standing metal wire-grid polarizer[11] shows low loss but the fabrication of high quality of the structure is challenging. A THz single layer wire-grid polarizer (SWGP) on silicon substrate was fabricated by Yamada *et al.*[10], with extinction ratio better than 23 dB in 0.5–3.0 THz, but high Fresnel surface loss is induced resulting in low transmittance because of high dielectric constant of Si substrate. To overcome this shortcoming, the SWGPs fabricated on different low absorption and low dielectric constant polymer substrates have been reported[12–15]. To further improve the extinction ratio, bilayer wire-grid polarizer (BWGP) was proposed and numerically analyzed[16]. A BWGP composed of two self-complementarily aligned gratings fabricated on one side of Si substrate was recently reported by Deng *et al.*[17], an average extinction ratio of 69.9 dB in 0.6–3 THz frequency range was achieved. But it suffered from low transmittance (only about 45%). Both high extinction ratio and high transmittance can be achieved with a thin-film BWGP, but the fabrication is quite complicated[18].

In this letter, a broadband THz polarizer consisting of two subwavelength metallic gratings on both sides of polyimide (PI) film is studied theoretically, and realized by a simple technique of laser induced and non-electrolytic plating with copper. High transmittance (over 67%) and high extinction ratios over 45 dB in 0.2–1.6 THz range of BWGPs are demonstrated.

Figure 1 shows the cross section of BWGP operated at THz range. BWGP consists of two metal wire grids or subwavelength metallic gratings on both sides of the substrate. Both gratings are of same parameters and parallel to each other, except there is lateral shift between two gratings. The flexible material called PI[19] is chosen as a substrate due to its low absorption and low dielectric constant in THz band. Copper grating is chosen due to our fabrication method, and also for its high electrical conductivity. Parameters p and w as shown in Fig. 1 represents the grating period and the width of the copper line. The fill factor is defined as the ratio of the width of copper wire to grating period ($f = w/p$), the thicknesses of PI and copper wire are t and h, respectively. For comparison, SWGP is easily obtained by removing one of metallic gratings from BWGP.

The transmissions of transverse magnetic (TM) wave and transverse electric (TE) wave for SWGP and

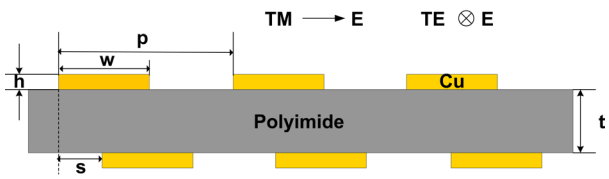

Fig. 1. (Color online) Cross section of BWGP.

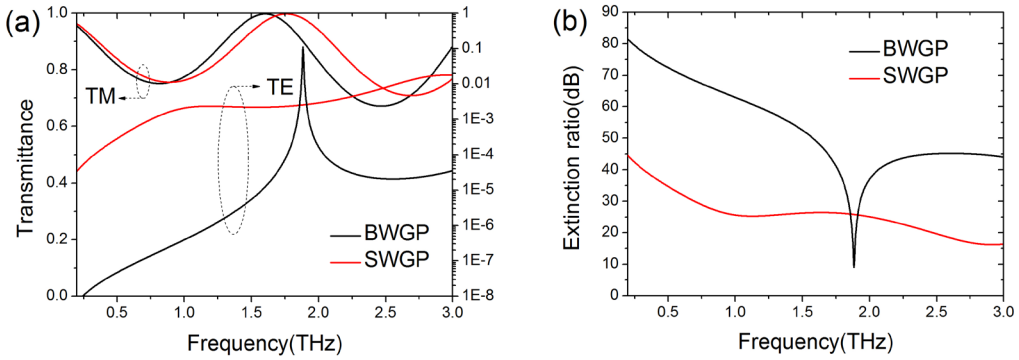

Fig. 2. (Color online) Comparison of SWGP and BWGP with lossless substrate: (a) TM and TE transmittances and (b) transmission extinction ratio.

BWGP at normal incidence are simulated by the finite-difference time-domain (FDTD) method (CST Microwave Studio). The thickness of copper $h = 1$ μm and its conductivity is set to 5.8×10^7 S/m. The grating period $p = 18$ μm, and the width of copper wire $w = 9$ μm, therefore, the fill factor is 0.5. The lateral shift is set to 0, that is, the two wire-grid structures are symmetrically distributed in both sides of the substrate. The lossless substrate with dielectric constants of 2.9 and 45 μm thickness is firstly assumed.

The simulated transmittances of TM and TE waves ($T_{\rm TM}$, $T_{\rm TE}$) for SWGP and BWGP in the frequency range from 0.2 to 3 THz are shown in Fig. 2(a). On the one hand, the difference between the transmittances of TM wave for SWGP and BWGP is very small, both have obvious periodic characteristics which is caused by Fabry–Perot (F-P) interference of the polarizer. On the other hand, the transmittances of TE wave for SWGP and BWGP rise with increasing frequency in general, due to the reducing ratio of wavelength to grating period[17]. In addition, the TE transmission of BWGP is over two orders of magnitude lower than that of SWGP in most frequencies. Therefore, the transmission extinction ratio which we defined as $10\times\log_{10}(T_{\rm TM}/T_{\rm TE})$ for BWGP is 20 dB higher than that for SWGP (Fig. 2(b)). However, the F-P interferences of TE waves in SWGP and BWGP are completely different. The TE transmission in BWGP appeared a strong narrow spike or cavity resonance near 1.88 THz. Thus, the transmission extinction ratio of BWGP drops rapidly to about 10 dB at resonant frequency, which greatly reduces the performance of BWGP or restricted its working frequencies. But this is not observed in the TE transmission in SWGP, that is, BWGP cannot be simply regarded as the stack of two SWGPs.

To further understand the cavity resonance of TE wave in BWGP, the TM, TE transmittances and the extinction ratio at different substrate thicknesses are simulated and shown in Fig. 3. It can be seen that the spike of TE wave moves to lower frequency as the thickness of the substrate increases. The resonant frequencies at different substrate thicknesses of 40, 45, and 50 μm are 1.70, 1.88, and 2.11 THz, respectively, which are slightly different from that calculated by F-P interference of the bare substrate without gratings. Because the magnetic response of the metallic grating does not exist, the transmission of TE wave and its resonant frequency can be calculated by equivalent refractive index model of Ref. [20]. But further physics of why this narrow resonance only happens for the TE transmission but not in TM transmission is still under investigation.

The influence of substrate loss on the performance of BWGP is also simulated (Fig. 4). In simulation, the dielectric constant of the substrate is set to 2.90+0.23i, which is close to that we used in the experiment. It is easy to see that the transmittance of TM wave has a certain

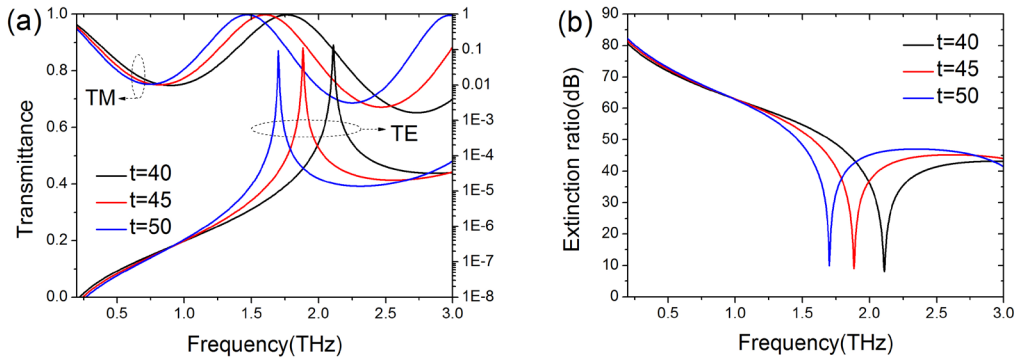

Fig. 3. (Color online) Influence of substrate thickness on BWGP performance: (a) TM and TE transmittances and (b) transmission extinction ratio.

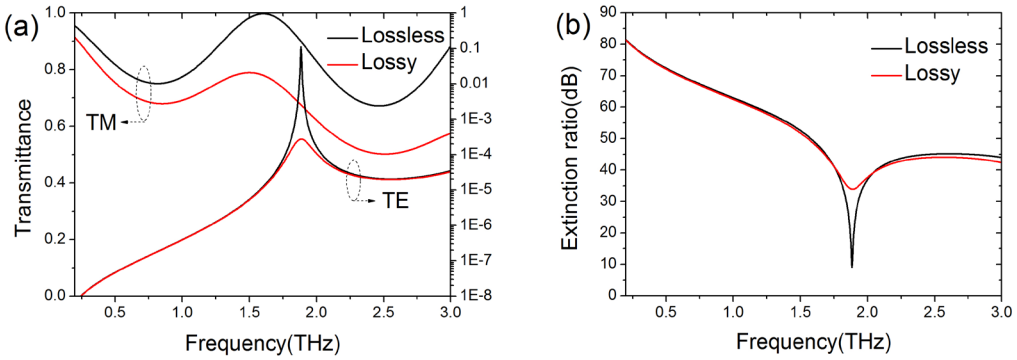

Fig. 4. (Color online) Comparison of BWGP with loss and lossless substrates: (a) TM and TE transmittances and (b) transmission extinction ratio.

degree of decline because of the substrate absorption. But, surprisingly we find that the interference spike of TE wave is significantly reduced, about three orders of magnitude smaller than that in lossless case. Thus, the transmission extinction ratio in lossy substrate is remarkably increased to 34 dB, which is 10 dB in lossless case at resonant frequency of 1.88 THz. To some extent, we can say that the absorption of the substrate is benefit for the broadband use of such kind of BWGP.

The influence of lateral shift s between two layers of gratings on the performance of BWGP is further investigated. Figure 5 shows the transmission extinction ratio of BWGP with lossless substrate under different s of 0, 4.5, and 9 μm (the results for lossy case are very similar and not figured out here). It can be seen that the extinction ratios of BWGP at three different lateral shifts are almost the same (<0.1 dB small changes). It is worth noting that the lateral shift almost has no effect on the transmission of TM wave. Therefore, the influence of lateral shift on the performance of BWGP can be ignored, which greatly reduces the difficulty of the BWGP fabrication.

The proposed BWGP is fabricated by a simple technique of laser induced and non-electrolytic plating with copper[14]. This technique mainly includes two steps, the first step is to obtain silver line with a few nanometer thicknesses using laser direct writing on $AgNO_3$ sol. The second is that the copper is deposited on silver seed by chemical reduction using non-electrolytic plating. Thanks for the transparency of the PI film in the visible region, the quality of being parallel between two metallic gratings in different sides of the substrate is easily adjusted with the help of charge coupled device camera illuminated by a red light-emitting diode lamp. Three BWGP samples at different lateral shifts as in Fig. 5 are fabricated on the PI film with a thickness of 45 μm and size of 1×1 (cm). The copper thickness is about 1.0 μm which is measured by Dektek150 step profiler. The transmissions of TM and TE waves are measured by using THz time-domain spectroscopy (THz-TDS) under dry nitrogen condition. Figure 6(a) shows the experimental results of TM and TE transmittances, and the simulation results are also shown with lossy substrate. Due to the sharply decreased signal-to-noise ratio (SNR) beyond 1.6 THz of THz-TDS used in the experiment, the test data after 1.6 THz are not included. Considering that the results for three polarizers are almost similar, only one is figured out.

The TM transmittance exceeding 67% in 0.2–1.6 THz is measured, and is obviously better than that of Si-based THz wire-grid polarizers[10,17] (45%), a little bit lower than that of high-density polyethylene (HDPE)-based wire-grid polarizer[12] (approximately 80%). This is mainly due to lower permittivities of PI and HDPE (2.9 and 2.4, respectively) than that of silicon (11.56) resulting in lower Fresnel surface loss. The transmission extinction ratio of the polarizer is shown in Fig. 6(b). It can be seen that the extinction ratio is higher than 45 dB and the average extinction ratio reaches 53 dB which is much better than that for SWGP[12–14]. There is large deviation between simulated and measured extinction ratios in lower frequencies, which may be caused by low SNR of measurement system. The limitation of the copper wire width for our fabricating technique is about 10 μm. To further improve the extinction ratio, one should choose smaller grating period and larger fill factor[16].

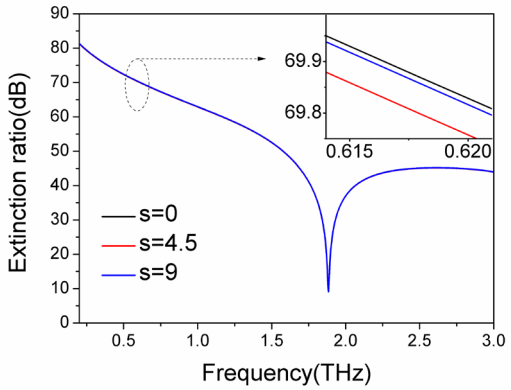

Fig. 5. (Color online) Simulations of BWGP performance at different lateral shifts.

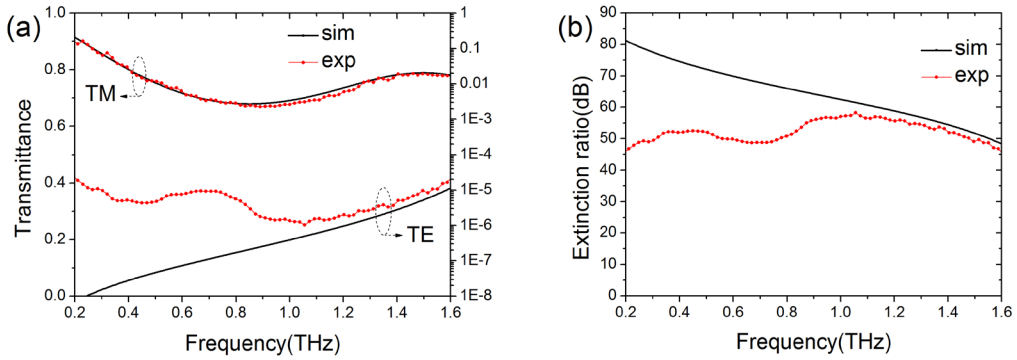

Fig. 6. (Color online) Comparison of BWGP performance for experiment and simulation: (a) TM and TE transmittances and (b) transmission extinction ratio.

In conclusion, a THz broadband using bilayer subwavelength metal wire-grid structure on both sides of PI film is simulated by the FDTD method. We analyze the effect of film thickness, material loss, and lateral shift between two layers of gratings on the performance of the THz polarizer. The structure is fabricated by a simple way of laser induced and non-electrolytic plating with copper. The performance of the BWGP is measured by THz-TDS system. High transmittance (over 67%) and high extinction ratios over 45 dB in 0.2–1.6 THz range of BWGPs are demonstrated. This kind of THz polarizer can be used both in continuous wave and in pulsed THz systems.

This work was partly supported by the National Natural Science Foundation of China under Grant Nos. 61377108 and 61107042.

References

1. M. Tonouchi, Nat. Photon. **1,** 97 (2007).
2. J. B. Baxter and G. W. Guglietta, Anal. Chem. **83,** 4342 (2011).
3. D. M. Mittleman, M. Gupta, R. Neelamani, R. G. Baraniuk, J. V. Rudd, and M. Koch, Appl. Phys. B **68,** 1085 (1999).
4. J. F. O'Hara, R. Singh, I. Brener, E. Smirnova, J. Han, A. J. Taylor, and W. Zhang, Opt. Express **16,** 1786 (2008).
5. A. Sell, A. Leitenstorfer, and R. Huber, Opt. Lett. **33,** 2767 (2008).
6. J. Wang, S. Wang, R. Singh, and W. Zhang, Chin. Opt. Lett. **11,** 011602 (2013).
7. A. K. Azad, H. T. Chen, X. Lu, J. Gu, N. Weisse-Bernstein, E. Akhadov, A. J. Taylor, W. Zhang, and J. F. O'Hara, Terahertz Sci. Technol. **2,** 15 (2009).
8. A. Wojdyla and G. Gallot, Opt. Express **19,** 14099 (2011).
9. C. F. Hsieh, Y. C. Lai, R. P. Pan, and C. L. Pan, Opt. Lett. **33,** 1174 (2008).
10. I. Yamada, K. Takano, M. Hangyo, M. Saito, and W. Watanabe, Opt. Lett. **34,** 274 (2009).
11. A. E. Costley, K. H. Hursey, G. F. Neill, and J. M. Ward, J. Opt. Soc. Am. **67,** 979 (1977).
12. Y. Ma, A. Khalid, T. D. Drysdale, and D. R. Cumming, Opt. Lett. **34,** 1555 (2009).
13. Z. Huang, H. Park, E. P. Parrott, H. P. Chan, and E. P. MacPherson, IEEE Photon. Technol. Lett. **25,** 81 (2013).
14. W. T. Wang, J. J. Liu, X. J. Li, H. Han, and Z. Hong, Acta Opt. Sin. **32,** 1231002 (2012).
15. M. Zhang, X. Li, S. Liang, P. Liu, J. Liu, and Z. Hong, Chin. Opt. Lett. **11,** 122301 (2013).
16. L. Sun, Z. H. Lv, W. Wu, W. T. Liu, and J. M. Yuan, Appl. Opt. **49,** 2066 (2010).
17. L. Y. Deng, J. H. Teng, L. Zhang, Q. Y. Wu, H. Liu, X. H. Zhang, and S. J. Chua, Appl. Phys. Lett. **101,** 011101 (2012).
18. Z. Huang, E. P. J. Parrott, H. Park, H. P. Chan, and E. Pickwell-MacPherson, Opt. Lett. **39,** 793 (2014).
19. H. Tao, A. C. Strikwerda, K. Fan, C. M. Bingham, W. J. Padilla, X. Zhang, and R. D. Averitt, J. Phys. D: Appl. Phys. **41,** 232004 (2008).
20. H. T. Chen, J. Zhou, J. F. O'Hara, F. Chen, A. K. Azad, and A. J. Taylor, Phys. Rev. Lett. **105,** 073901 (2010).